



Title	EFFECT OF BAR CUTOFF ON THE ARCH AND CATENARY ACTIONS OF RC BEAMS UNDER GRAVITATIONAL LOADINGS
Author(s)	TSAI, MENG-HAO; LU, JUN-KAI; HUANG, BO-HONG
Citation	Proceedings of the Thirteenth East Asia-Pacific Conference on Structural Engineering and Construction (EASEC-13), September 11-13, 2013, Sapporo, Japan, D-6-4., D-6-4
Issue Date	2013-09-12
Doc URL	http://hdl.handle.net/2115/54337
Type	proceedings
Note	The Thirteenth East Asia-Pacific Conference on Structural Engineering and Construction (EASEC-13), September 11-13, 2013, Sapporo, Japan.
File Information	easec13-D-6-4.pdf



[Instructions for use](#)

EFFECT OF BAR CUTOFF ON THE ARCH AND CATENARY ACTIONS OF RC BEAMS UNDER GRAVITATIONAL LOADINGS

Meng-Hao Tsai^{*†}, Jun-Kai Lu, and Bo-Hong Huang

Department of Civil Engineering Department, National Pingtung University of Science and Technology, Taiwan

ABSTRACT

Static loading tests on six RC beam-column sub-assemblages were carried out in this study to investigate the effect of bar layout on the collapse resistance of a two-span beam, which was defined as the continuous beam bridging over a suddenly failed interior column of a building frame. Experimental results indicated that the contribution of compressive arch and catenary actions to collapse resistance was influenced by the bar cutoff in the spans. The beam-end compressive bars had a moderate contribution to the arch resistance under column loss even if they were cut off in the mid-span. An appropriate amount of compressive bars at the beam-end region helped to mitigate the degradation of arch resistance in transition phase. However, the compressive bars that were cut off in the mid-span region failed to provide catenary force under large deflection. They should be conservatively neglected in the estimation of catenary force. If development of the catenary action is expected in structural design, it is better to reduce the amount of bars that are simultaneously cut off in the two-span beam. Based on the test results, the bar layout dominated by gravitational and seismic loading design may be appropriately revised to have a more satisfactory performance against sudden column loss.

Keywords: RC sub-assemblage, arch action, catenary action, bar cutoff, collapse resistance.

1. INTRODUCTION

Development of practical and efficient approaches for protecting building structures from progressive collapse under accidental column loss has been an imperative issue in the past decade. In general, tie force, alternative load path, integrity provisions, and specific local load resistance are recommended as feasible measures for reducing the vulnerability of building structures to progressive collapse (Abruzzo *et al.* 2006, Ellingwood 2006, Mohamed 2006, Nair 2006). Since the cause, reoccurrence, and intensity of abnormal loadings for triggering the progressive collapse are difficult to predict precisely, providing alternate loading paths has become an acceptable and popular solution. Provision of reliable alternate loading paths usually depends on the integrity,

* Corresponding author: Email: mh-tsai@mail.npust.edu.tw

† Presenter: Email: mh-tsai@mail.npust.edu.tw

redundancy, and strength of the remaining structural members. The two-span beam bridging over the failed column may be regarded as the most important role to redistribute the supporting loadings. In conventional structural design and analysis, pure bending capacity has been used to define the flexural strength of beam members. Nevertheless, it is known that compressive arch and tensile catenary actions may be developed under gravitational loading if the beam ends are appropriately restrained.

Some experiments have been conducted with beam-column sub-assemblages. [Su *et al.* \(2009\)](#) conducted static vertical loading tests on twelve longitudinally restrained RC beams with varied steel ratios and span-to-depth ratios. The tested specimens generally reached peak compressive arch strength at a deflection ranging from 16% to 34% of section depth. The load resistance in catenary stage may be lower than the arch strength. [Sasani and Kropelnicki \(2008\)](#) and [Sasani *et al.* \(2011\)](#) adopted a 3/8 scaled sub-assemblage to investigate the column-loss response of an RC beam bridging over the removed column. [Choi and Kim \(2011\)](#) performed static loading tests on reduced-scale RC sub-assemblages designed with and without seismic detailing and concluded that significant catenary action may be activated for seismically detailed beams. From these evidences, it is recognized that experimental studies are important and necessary to clarify the column-loss response of various member details.

In practical engineering, flexural reinforcements of RC beams may be cut off at appropriate locations as long as the remaining steel bars are sufficient to provide the required moment resistance. This makes the steel ratio may vary along the spans. Hence, experimental investigation for the effect of bar cutoff on the column-loss response of RC members was conducted in this study. Monotonic static loading tests on six beam-column sub-assemblages designed with different bar cutoff patterns were carried out. Load-displacement response and restraint forces were measured to evaluate the influence of bar cutoff on the column-loss response. Practical considerations for the progressive collapse resistance of RC members with bar cutoff were provided.

2. DESIGN OF TEST SPECIMENS AND EXPERIMENTAL SETUP

2.1. Test Specimens

Six sub-assemblage specimens were designed with varied reinforcement ratios and bar cutoff locations. Dimensions of the test specimens were determined with reference to the design drawings of a real ten-story RC building frame ([Tsai and Huang 2013](#)). Section dimensions of the two-span beam were 200 mm in width and 250 mm in depth. The span-to-depth ratio was 6.4 with a clear span length equal to 1600 mm. Section dimensions of the column stubs were 300 mm in width and 400 mm in depth. Main reinforcements of the S1 and S2 sub-assemblages were continuous with constant steel ratios, as shown in [Figure 1\(a\)](#). They were respectively considered as the benchmark specimen with strong and weak flexural strength. For the rest sub-assemblages, the main reinforcements were cut off at some predetermined locations. Detailed bar cutoff locations of those

specimens, which were designated as C1, C2, C3, and C4, are shown in [Figure 1\(b\)](#). The bar arrangement of C1 was defined as V-type cutoff and considered as a gravitational-controlled design, while that of C2 was defined as X-type cutoff and considered as a seismic-controlled design. C3 and C4 were respectively defined as K-type and Z-type cutoff. Bar layouts and characters of the specimens are summarized in [Table 1](#). Meanwhile, ten #7 steel bars were used as the main reinforcements for all column sections. They were confined with #5 shear stirrups spaced at 100 mm. The significantly larger moment strength of column sections ensured that plastic hinges were restricted to the two-span beam member. Design yield stress was 275 MPa for steel reinforcements not larger than #5 and 412 MPa for #7. Design compressive strength of concrete was 20.6 MPa.

2.2. Experimental Setup

[Figure 2\(a\)](#) shows a schematic drawing of the test setup. It is seen that each side column of the sub-assembly was bolted to a reaction seat made of H488x300 and H300x300 steel sections. The reaction seat was connected to the strong ground floor through two bi-axial load cells, which were used to measure the horizontal and vertical reactions. They were used to estimate the axial forces of the two-span beam. Displacement response at the mid-span and the middle column stub were measured by position transducers. Relative deflection between the middle column stub and the mid-span was used to calculate the chord rotation of the two-span beam. Twelve strain gauges were distributed in the east span of the sub-assembly. Detailed instrumentation of the gauges and sensors is also shown in [Figure 2\(a\)](#). A typical failure mode of the test specimens is shown in [Figure 2\(b\)](#).

3. TEST RESULTS

[Figure 3\(a\)](#) presents the vertical load-displacement response curves of the S1, S2, C2, and C4 specimens. It is seen that the applied loading quickly climbed up under small deflection. Then, it decreased with increased deflection and started to climb again as the deflection was larger than about 240 mm. Their corresponding horizontal reactions are shown in [Figure 3\(b\)](#), where negative forces indicate that the specimens were subjected to axial compression. Based on the variation of horizontal reactions, the response in [Figure 3\(a\)](#) may be divided into three phases. The first one is the compressive arch phase, which ranges from the start to the peak compressive reaction. The second one is the catenary phase, which covers the range with tensile reaction. The final one is defined as the transition phase, which is between the former two phases.

It is observed that S1, C2, and C4 specimens had approximately equal response at the very beginning of the loading process. Due to less compressive bars at the beam ends, the load response of C4 descended first with a steeper trend. The C2 specimen displayed a more similar arch response to S1. This revealed that an appropriate amount of compressive bars at the beam-end region helped to mitigate the reduction of arch resistance. However, the load response of C2 still declined faster than the S1 and S2 specimens because of the cutoff of 50% main reinforcements in the mid-span

region. In [Figure 3\(b\)](#), the peak compressive reaction of S1 and S2 were approximately equal to that of C2 and C4, respectively. In general, their peak compressive reactions occurred at a deflection approximately equal to half of the section depth. Also, compressive reactions of S1 and C2 were larger than that of S2 and C4 because of more compressive bars provided in the former two specimens. In [Figure 3\(a\)](#), it is seen that the catenary action was activated at a displacement around 250 mm ~ 300 mm, which was close to the section depth. Except for C2, the loading resistance in the arch phase could be recovered during the catenary phase. It appeared that the catenary development was interrupted for the C2 specimen as 50% of the top and bottom reinforcements were simultaneously cut off in the mid-span region. C4 presented comparable catenary force to S1 even though 50% of its tensile steel bars were cut off at around one-third span. C2 appeared to have similar catenary response to C4 despite the premature bar rupture. Since the compressed concrete at the beam ends of C2 was crushed during the loading process, the curtailed bars lost enough bonding to develop tensile resistance. Therefore, the curtailed compressive bars of C2 had a minor contribution to the catenary force. On the contrary, the curtailed tensile bars should have moderate contribution in the catenary phase before bar fracture.

The vertical load-displacement response of S1, S2, C1, and C3 specimens are compared in [Figure 4\(a\)](#). It is seen that the response of C3 was approximately equal to that of S1. They even had similar variation of horizontal reactions as shown in [Figure 4\(b\)](#). This reveals that for a gravitational design beam, if the curtailed tensile bars of the mid-span region were extended into the joint with the failed column, its collapse resistance could be significantly enhanced. In fact, even the curtailed bottom reinforcement of the seismic-controlled bar layout in the C2 specimen could be extended to the mid-span to resemble the K-type cutoff in C3. On the other hand, the S2 and C1 specimens presented similar load-displacement response in the catenary phase. Because of more compressive bars at the interior beam ends, C1 induced larger compressive reactions than the S2 specimen, as shown in [Figure 4\(b\)](#). Also, the positive moment strength at the interior beam ends of C1 was less than the negative moment strength at the exterior beam ends. Hence, the plastic hinges appeared at the interior beam ends first. This would reduce the catenary action of the C1 specimen such that it induced less tensile reactions than S2. These evidences imply that the curtailed compressive bars at the interior beam ends and the curtailed bottom bars at the mid-span of the C1 specimen had negligible influence on the catenary resistance.

4. CONCLUSIONS

An experimental study was carried out to investigate the influence of different bar layouts on the collapse resistance of beam-column sub-assemblages. Test results indicated that the beam-end compressive bars had a moderate contribution to the arch resistance under column loss even if they were cut off in the mid-span. An appropriate amount of compressive bars at the beam-end region helped to mitigate the reduction of arch resistance. However, if the compressive bars were cut off in the mid-span region, they could not effectively provide catenary force under large deflection. This

implied that they should be conservatively neglected in the estimation of catenary force. Hence, the gravitational-controlled bar layout resulted in similar catenary response to the layout with continuous bars only. Nevertheless, collapse resistance of the gravitational-controlled cutoff could be significantly improved if the curtailed bottom bars were extended into the joint with the failed column. Similarly, the seismic-controlled cutoff could resemble the preferable cutoff if the curtailed bottom bars were extended to the mid-span. This suggests that if the arch and catenary action were expected in the progressive collapse resistant design, the bottom bars at the beam ends connected with the failed column should be extended at least into the mid-span and appropriate amounts of compressive bars should be provided.

5. ACKNOWLEDGMENTS

This study was supported by the National Science Council of Taiwan through grant No. NSC 100-2628-E-020-021-MY3. The support is gratefully acknowledged. Assistance from the National Research Center for Earthquake Engineering (NCREE) in the experiment is also greatly appreciated.

REFERENCES

- Abruzzo J, Matta A, and Panariello G (2006). Study of mitigation strategies for progressive collapse of a reinforced concrete commercial building. *Journal of Performance of Constructed Facilities*, Vol. 20, pp.384-390.
- Choi H and Kim J (2011). Progressive collapse-resisting capacity of RC beam-column sub-assembly. *Magazine of Concrete Research*, Vol. 63, pp. 297-310.
- Ellingwood BR (2006). Mitigating risk from abnormal loads and progressive collapse. *Journal of Performance of Constructed Facilities*, Vol. 20, pp. 315-323.
- Mohamed OA (2006). Progressive collapse of structures: annotated bibliography and comparison of codes and standards. *Journal of Performance of Constructed Facilities*, Vol. 20, pp. 418-425.
- Nair RS (2006). Preventing disproportionate collapse. *Journal of Performance of Constructed Facilities*, Vol. 20, pp. 309-314.
- Sasani M and Kropelnicki J (2008). Progressive collapse analysis of an RC structure. *Structural Design of Tall and Special Buildings*, Vol. 17, pp. 757-771.
- Sasani M, Werner A, and Kazemi A (2011). Bar fracture modeling in progressive collapse analysis of reinforced concrete structures. *Engineering Structures*, Vol. 33, pp. 401-409.
- Su Y, Tian Y, and Song X (2009). Progressive collapse resistance of axially-restrained frame beams. *ACI Structural Journal*, Vol. 106, pp. 600-607.
- Tsai MH and Huang TC (2013). Progressive collapse analysis of an RC building with exterior partially infilled walls. *Structural Design of Tall and Special Buildings*, Vol.22, pp.327-348.

Table 1 Characteristics of the test specimens

Specimen	Bar layout	Character
S1	4#4 for both top and bottom	Strong flexural strength
S2	2#4 for both top and bottom	Weak flexural strength
C1 (V-type)	Top bars: 4#4 + 2#4 + 4#4 Bottom bars: 2#4 + 4#4 + 2#4	Gravitational-controlled design Effect of gravitational tensile bars
C2 (X-type)	Top bars: 4#4 + 2#4 + 4#4 Bottom bars: 4#4 + 2#4 + 4#4	Seismic-controlled design Effect of mid-span cutoff
C3 (K-type)	Top bars: 4#4 + 2#4 + 4#4 Bottom bars: 2#4 + 4#4 + 4#4	Comparison with C1 and S1
C4 (Z-type)	Top bars: 4#4 + 2#4 + 2#4 Bottom bars: 2#4 + 2#4 + 4#4	Comparison with S1 and S2

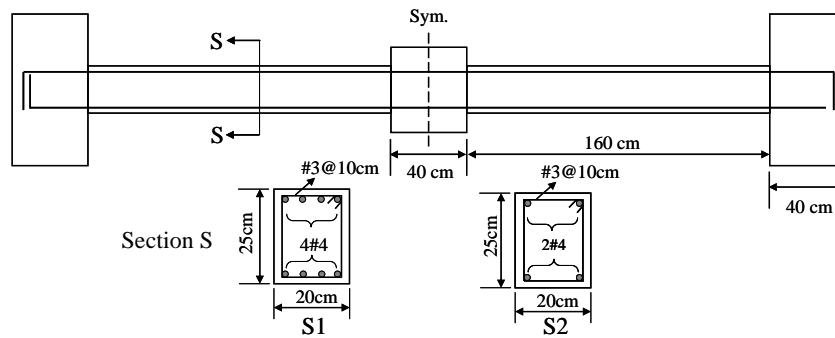


Figure 1(a) Design drawings of S1 and S2 sub-assemblages

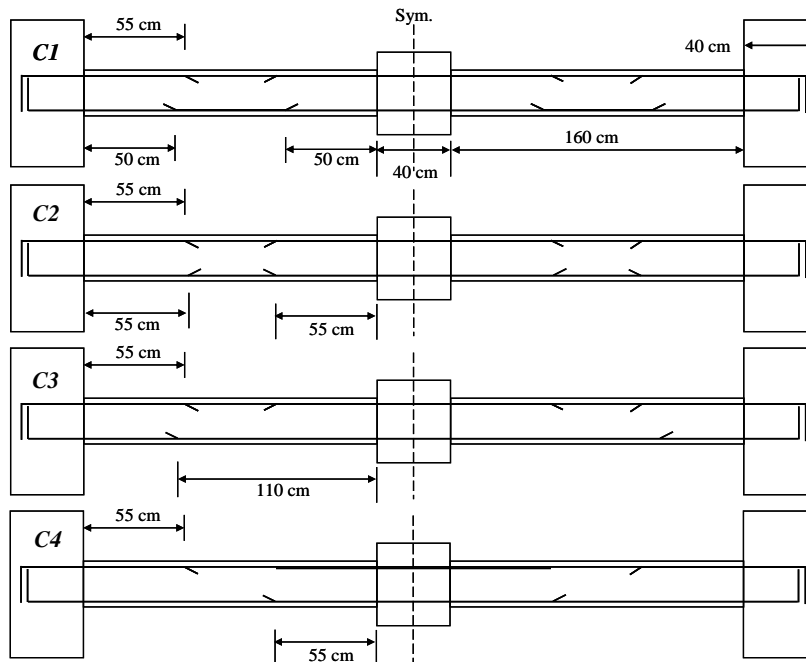


Figure 1(b) Design drawings of C1, C2, C3, and C4 sub-assemblages

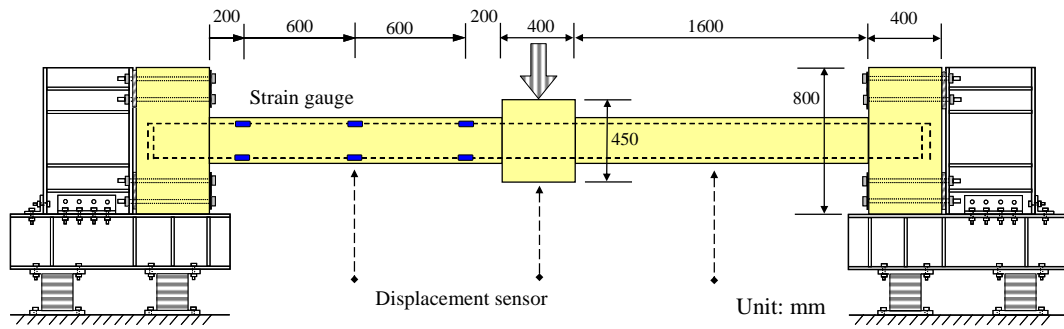


Figure 2(a) Test setup



Figure 2(b) A typical failure mechanism

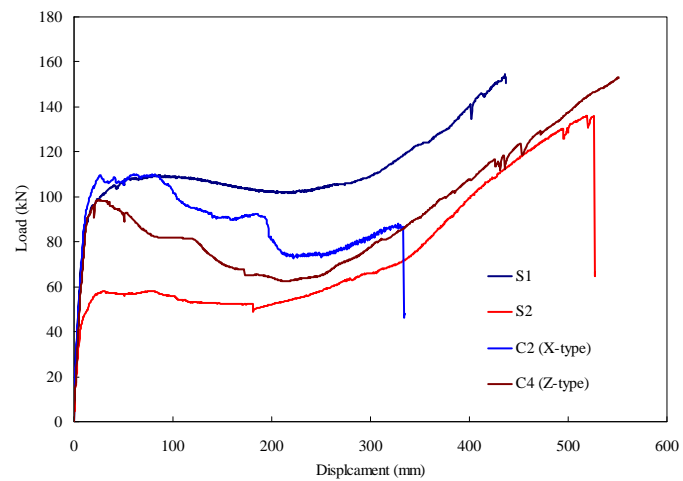


Figure 3(a) Load-displacement response of S1, S2, C2, and C4

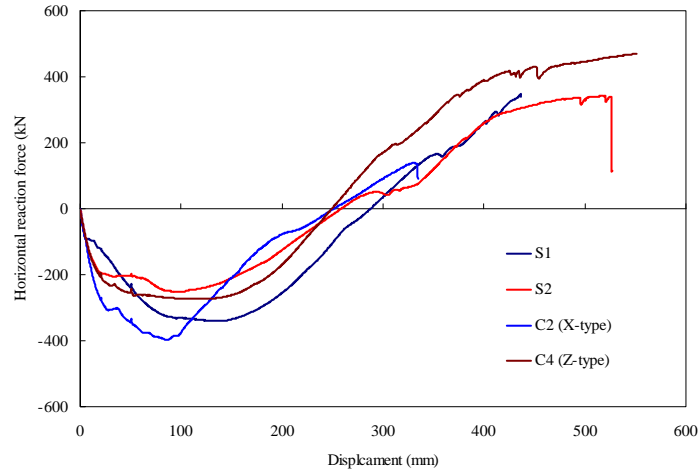


Figure 3(b) Horizontal reaction force of S1, S2, C2, and C4

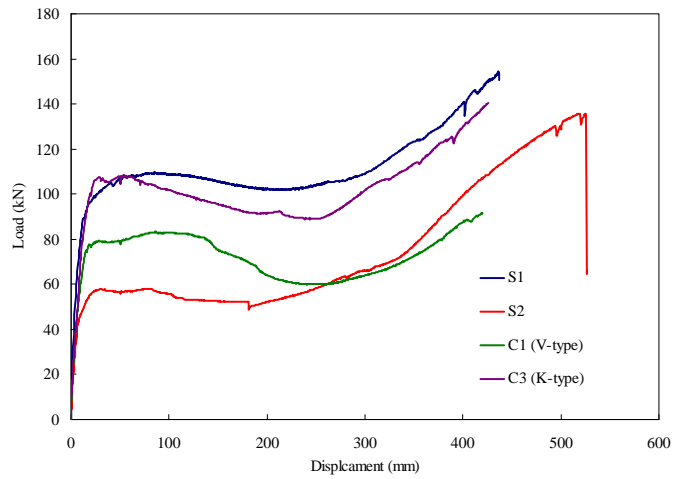


Figure 4(a) Load-displacement response of S1, S2, C1, and C3

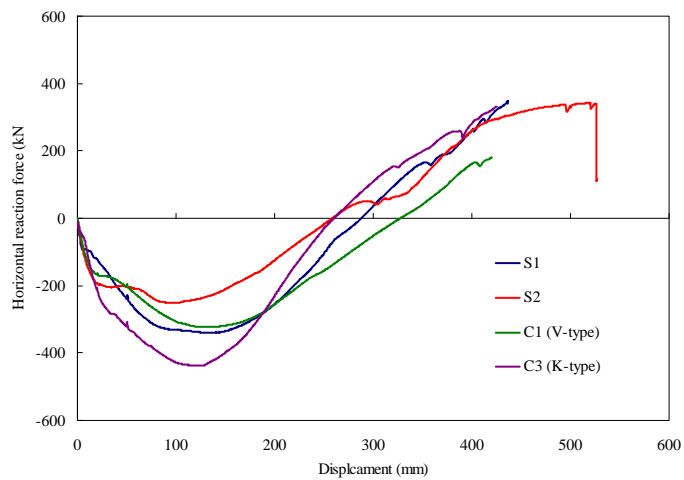


Figure 4(b) Horizontal reaction force of S1, S2, C2, and C4